Supporting Information for "Low-Frequency Earthquakes Accompany Deep Slow-Slip beneath the North Island of New-Zealand"

F. Aden-Antoniów[1,2], W.B. Frank[1], C.J. Chamberlain[3], J. Townend[3], L.M. Wallace[2,4], S. Bannister[2]

[1]Department of Earth, Atmospheric and Planetary Sciences, Massachusetts Institute of Technology, Cambridge, MA, USA

[2]GNS Science, Lower Hutt, New Zealand

[3]School of Geography, Environment and Earth Sciences, Victoria University of Wellington, Wellington, New Zealand

[4]University of Texas Institute for Geophysics, Austin, TX, USA

Contents of this file

Figures complementing information reported in the main text

References

Lomax, A., Virieux, J., Volant, P., & Berge-Thierry, C. (2000). Probabilistic earthquake location in 3d and layered models. In *Advances in seismic event location* (pp. 101–134). Springer.

Wallace, L. M., & Eberhart-Phillips, D. (2013). Newly observed, deep slow slip events at the central hikurangi margin, new zealand: Implications for downdip variability of slow slip and tremor, and relationship to seismic structure. *Geophysical Research Letters*, *40*(20), 5393–5398.

Williams, C. A., Eberhart-Phillips, D., Bannister, S., Barker, D. H., Henrys, S., Reyners, M., & Sutherland, R. (2013). Revised interface geometry for the hikurangi subduction zone, new zealand. *Seismological Research Letters*, *84*(6), 1066–1073.

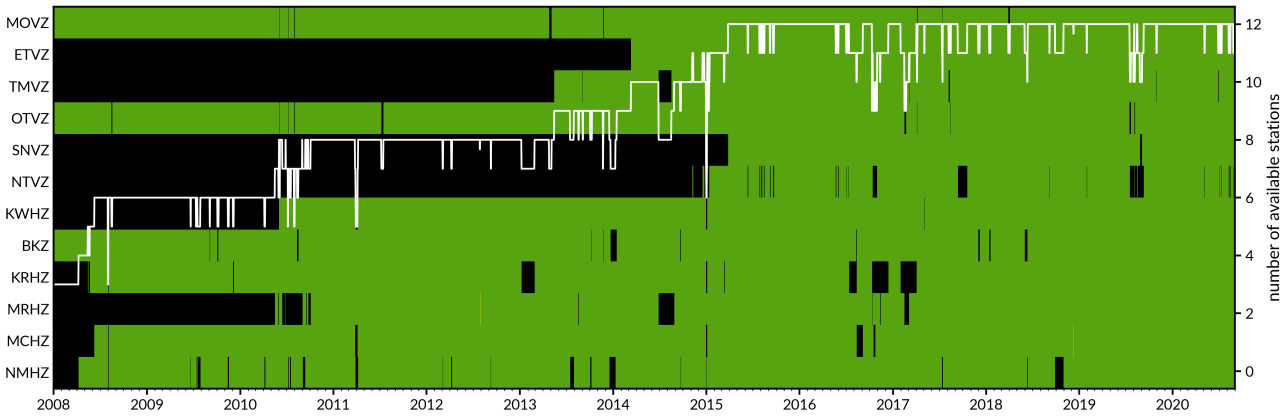

Figure S1. Example of a short synthetic catalog generated for this study. (left) Spatial distribution of the synthetic mainshocks (orange) and aftershocks (yellow). The black contours represent the 2D probability function use to generate the location of these earthquakes. (right) Cumulative number of the mainshocks and the aftershocks.

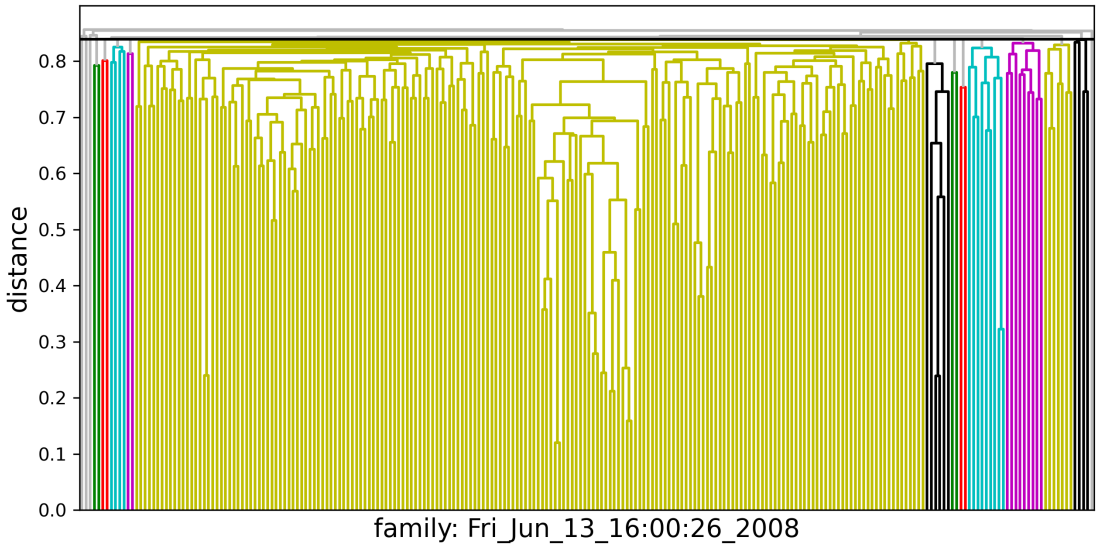

Figure S2. Example of a short synthetic catalog generated for this study. (left) Spatial distribution of the synthetic mainshocks (orange) and aftershocks (yellow). The black contours represent the 2D probability function use to generate the location of these earthquakes. (right) Cumulative number of the mainshocks and the aftershocks.

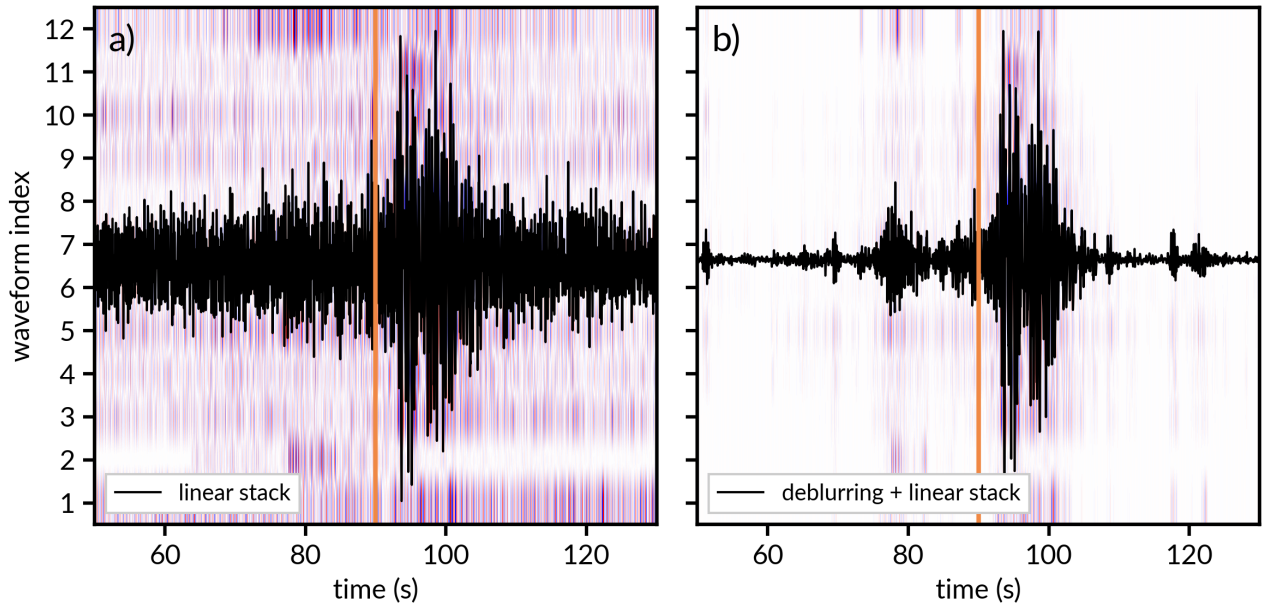

Figure S3. Example of a deblurring filter applied on a family. (a) The trace represent the linear stack of twelve detected events at a given station and component. The waveforms amplitudes are represented by the color palette. (b) The trace represent the linear stack of twelve detected events at a given station and component after the use of the deblurring filter with a sliding window of 100 samples (1 second). The waveforms amplitudes are represented by the color palette.

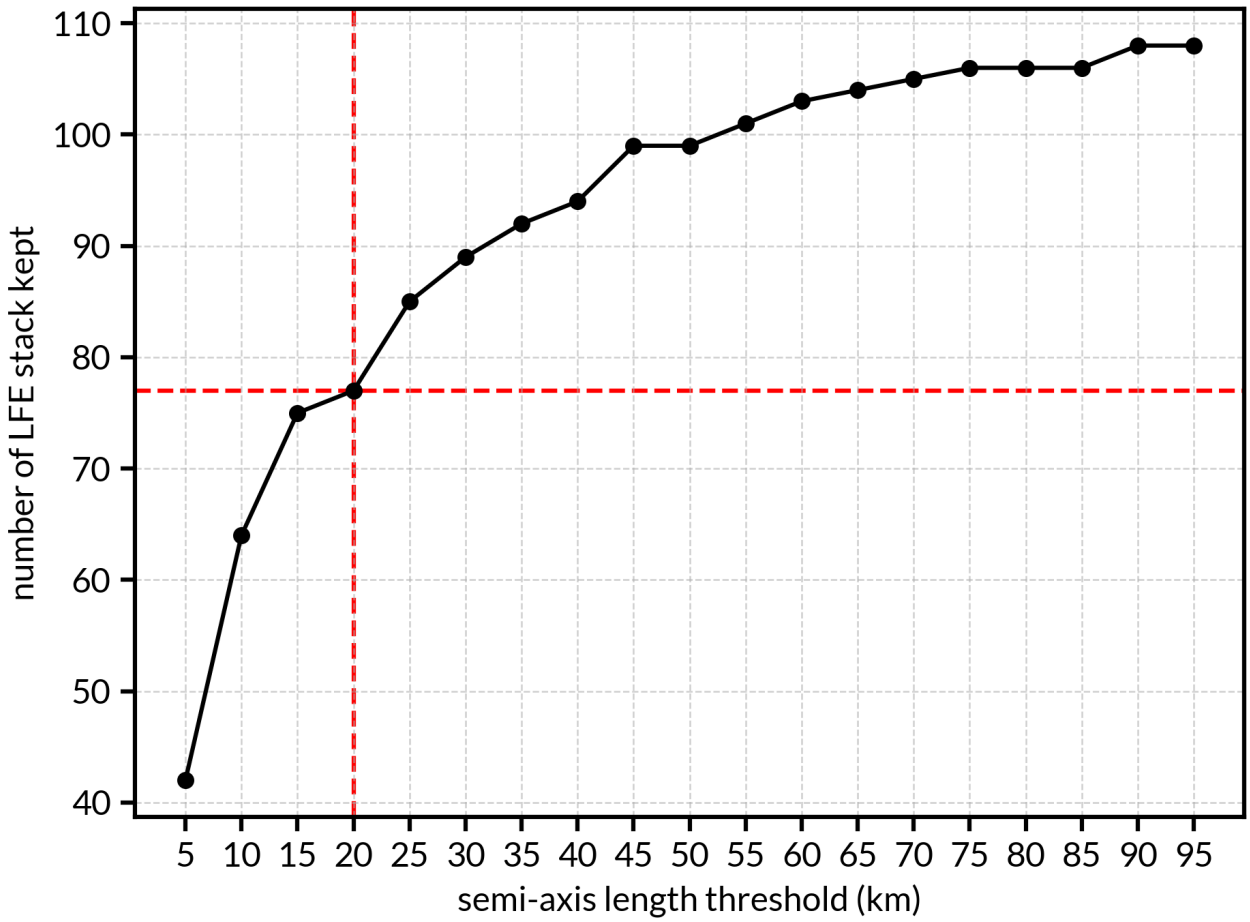

Figure S4. Number of LFE stack kept as a function of the 68% error ellipsoid semi-axis length threshold used. In this study we selected a threshold of 20km resulting in a catalog of 77 LFE stacks.

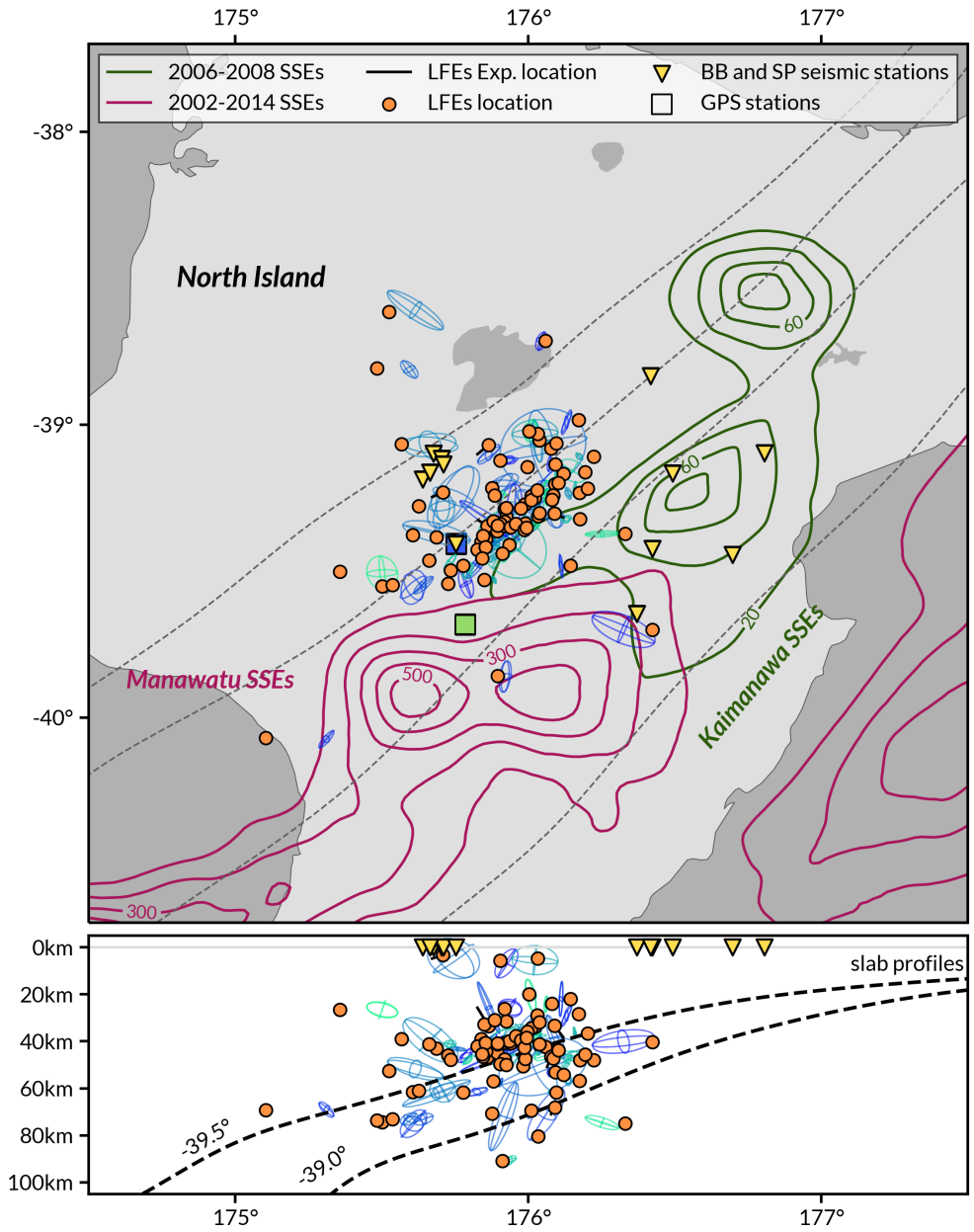

Figure S5. Spatial distribution of the LFE candidates. (top) map view representing the location of the candidates in orange with their 68% error ellipsoid obtained with NonLinLoc (Lomax et al., 2000). The colored contour lines mark the cumulative slip of the different Slow Slip Events occurring beneath the North Island since 2002 (Wallace & Eberhart-Phillips, 2013). (bottom) East-West profile representing the distribution of the LFE candidates at depth. The dashed lines represents different plate interface profile from Williams et al. (2013).

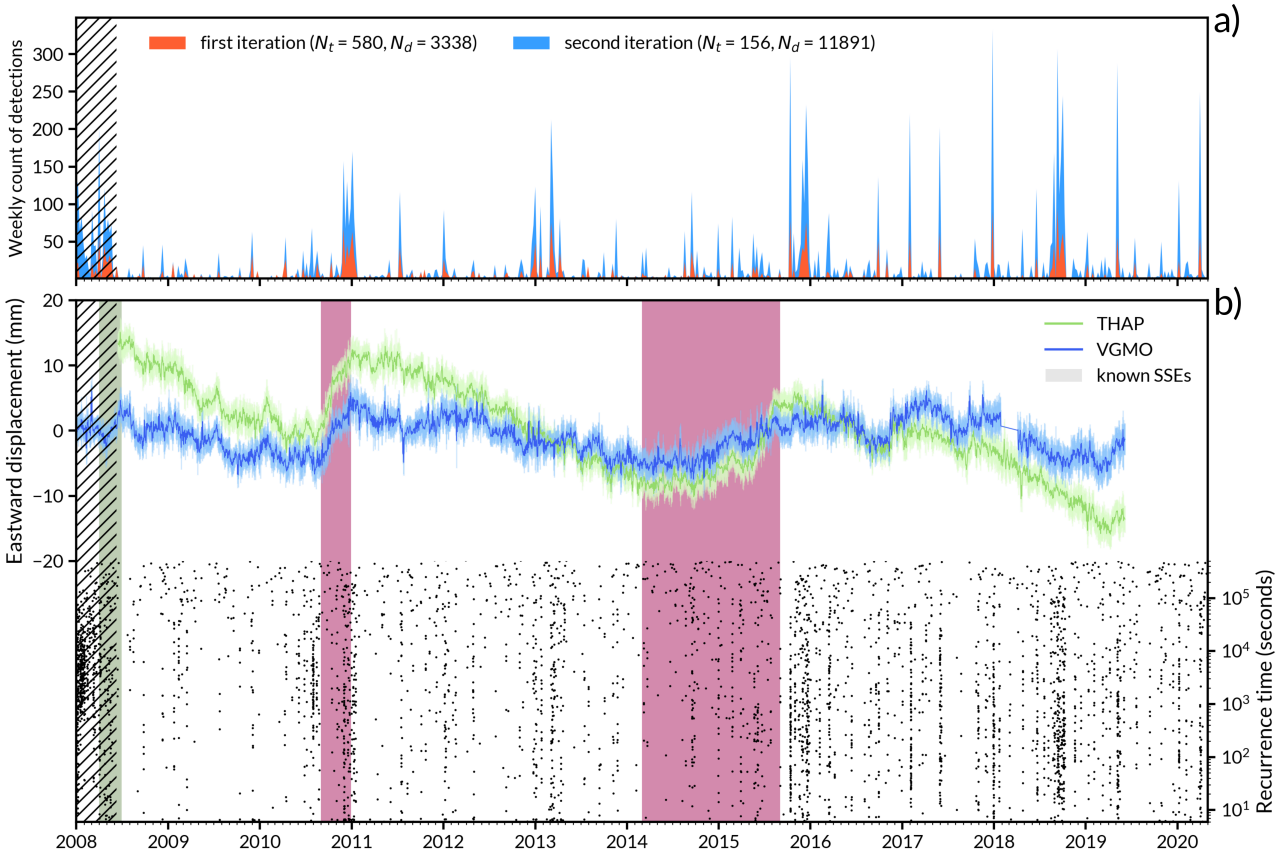

Figure S6. low-frequency earthquakes activity and GPS displacement. (a) The weekly detection counts for the two iteration of our iterative approach are shown in color with a matched-filter detection threshold set at 10 x Median Absolute Deviation of the cross-correlation time series. The hatched area correspond to a high detection rate related to a limited number of station available. (b) A comparison between GPS time series at tow stations (THAP and VGMO see Figure S4) and the recurrence time between consecutive events against the cumulative number of events (for all families) along time. The shaded area correspond to known slow slip Events and their color correspond to their location (see Figure S4).

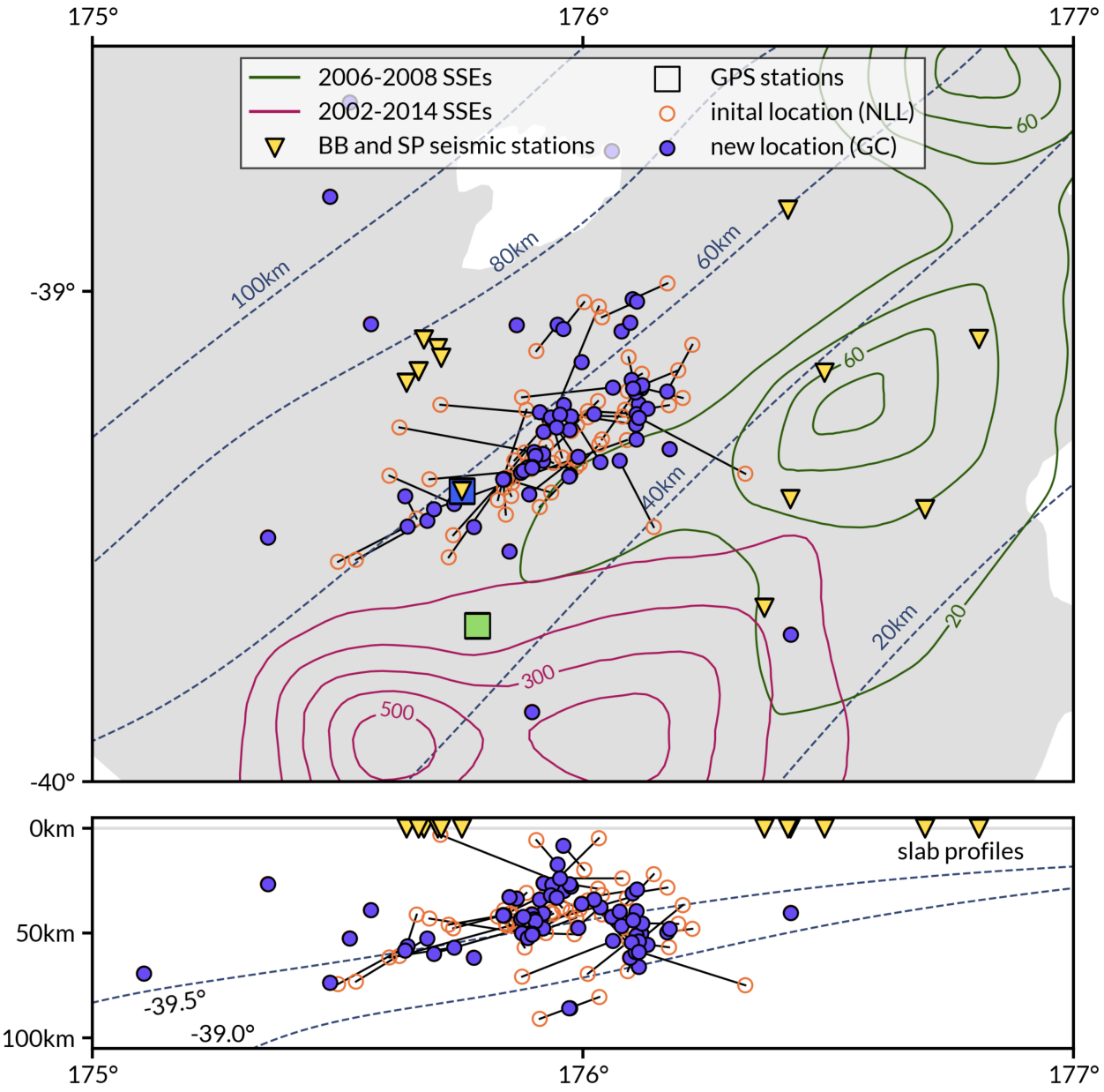

Figure S7. Relocation of the LFE candidates using GrowClust with a $r_{min} = 0.4$. The orginal location obtain with NonLinLoc is represented by the empty orange circles. The black lines show the distance between the initial and new location obtained with GrowClust and represented by purple circles. a) and b) show respectively a map and a profile view. The dashed lines represents different plate interface profile from Williams et al. (2013).

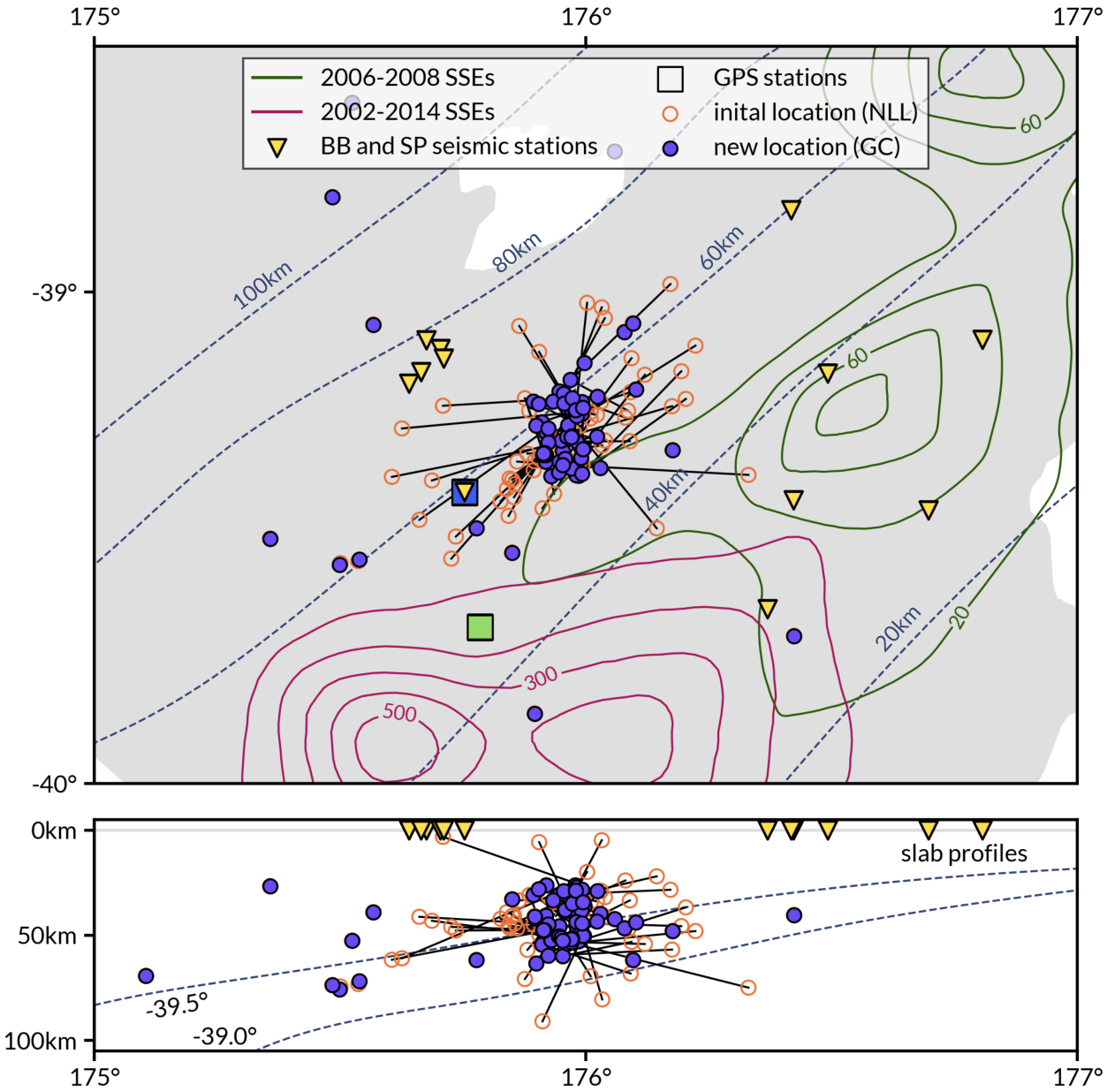

Figure S8. Relocation of the LFE candidates using GrowClust with a $r_{min} = 0.2$. Same as Figure S5.

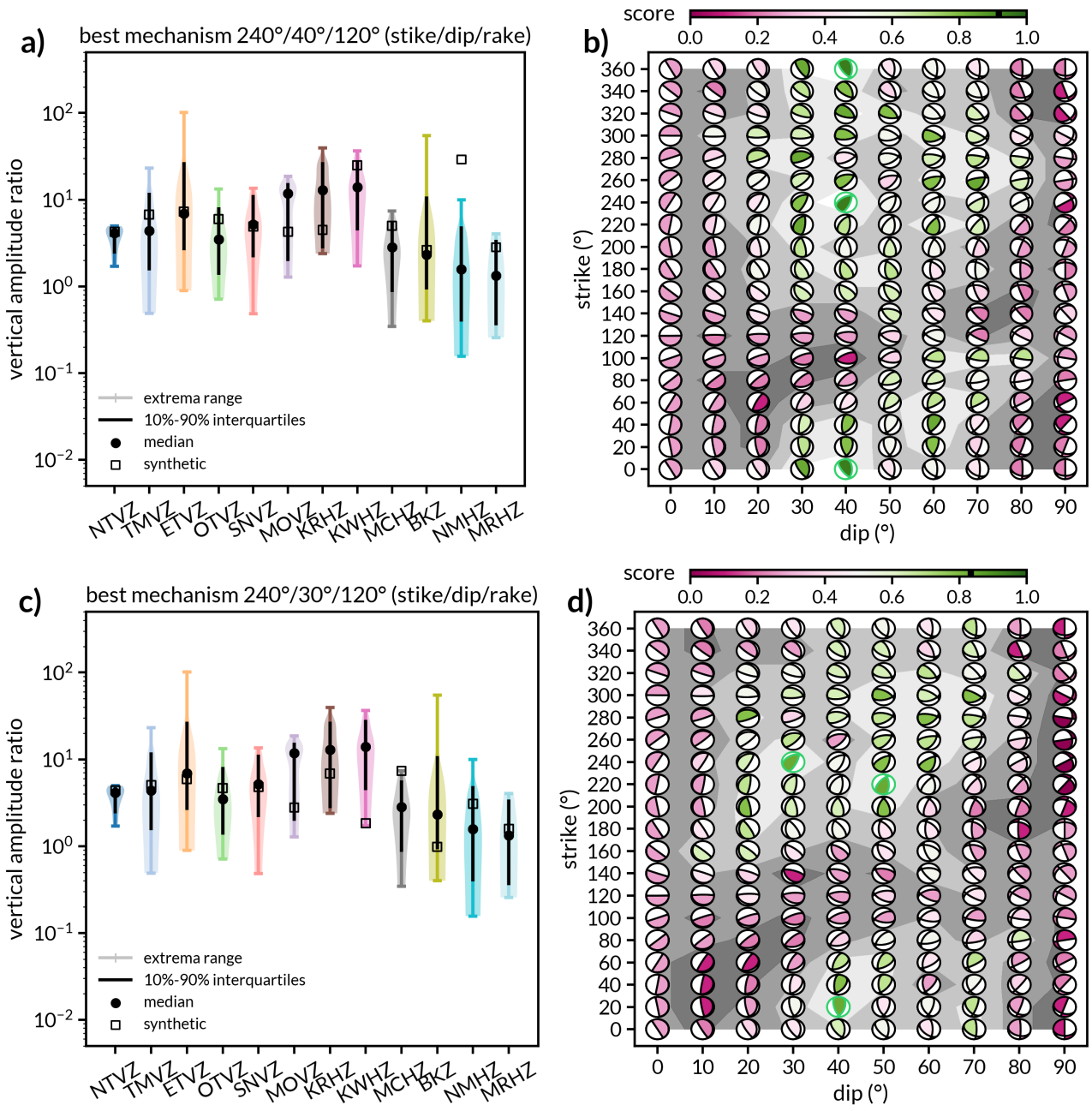

Figure S9. Representation of the score for different strikes and dips for a given rake of 90°and depth of 45 (a, b) and 55km (c, d). (a, c) Comparison of the S/P amplitude ratios at each station between the final low-frequency earthquakes templates (violins) and the synthetic waveforms assuming a the best fitting source mechanism. The score represents the percentage of synthetic amplitude ratios that fall into the 10%-90% interquartile range (IQR) of the observed distribution. (b, d) The green-outlined beachball represents the mechanism with the highest score. The background levels of gray show the distribution of the score with light colored areas representing higher scores.

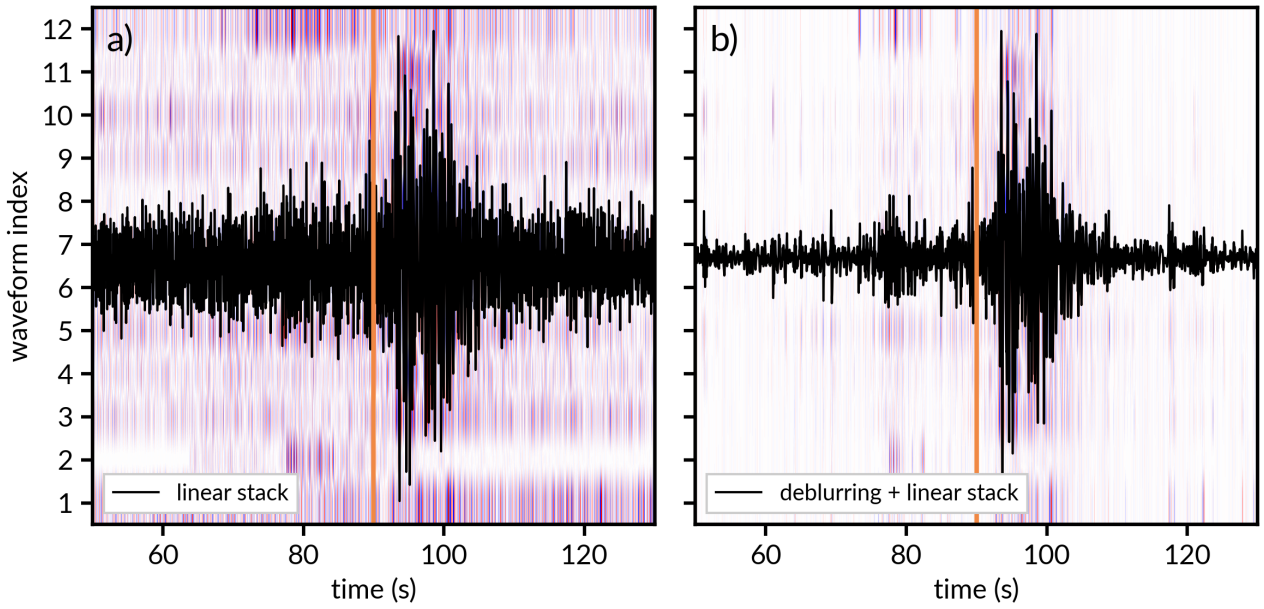

Figure S10. Example of a deblurring filter applied on a family. (a) The trace represent the linear stack of twelve detected events at a given station and component. The waveforms amplitudes are represented by the color palette. (b) The trace represent the linear stack of twelve detected events at a given station and component after the use of the deblurring filter with a sliding window of 25 samples (0.25 second). The waveforms amplitudes are represented by the color palette.

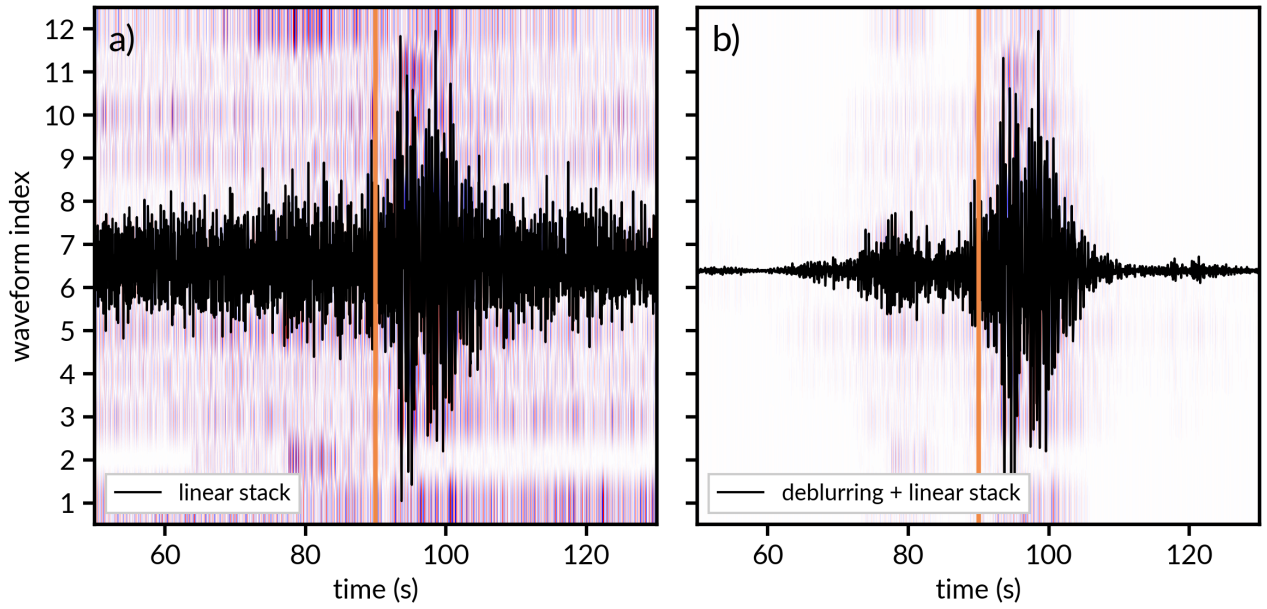

Figure S11. Example of a deblurring filter applied on a family. (a) The trace represent the linear stack of twelve detected events at a given station and component. The waveforms amplitudes are represented by the color palette. (b) The trace represent the linear stack of twelve detected events at a given station and component after the use of the deblurring filter with a sliding window of 1000 samples (10 seconds). The waveforms amplitudes are represented by the color palette.

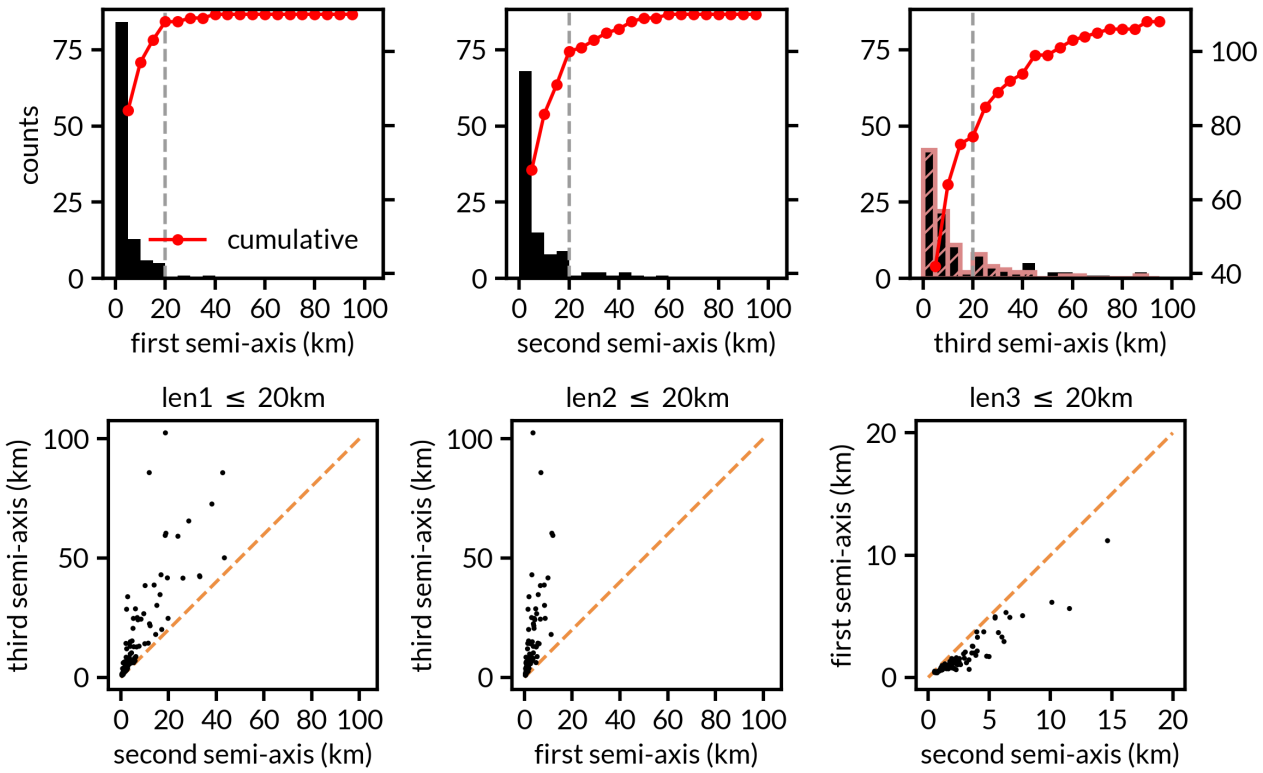

Figure S12. Distributions of the location 68% error ellipsoid given by NonLinLoc. (top) the distributions of each semi-axis length are shown in black, the cumulative number is shown in red. (top right) the red dashed histogram shows the distribution of the third semi-axis if the two firsts are lower or equal to 20km. (bottom) distribution of the remaining semi-axis when one is set to be lower or equal to 20km.

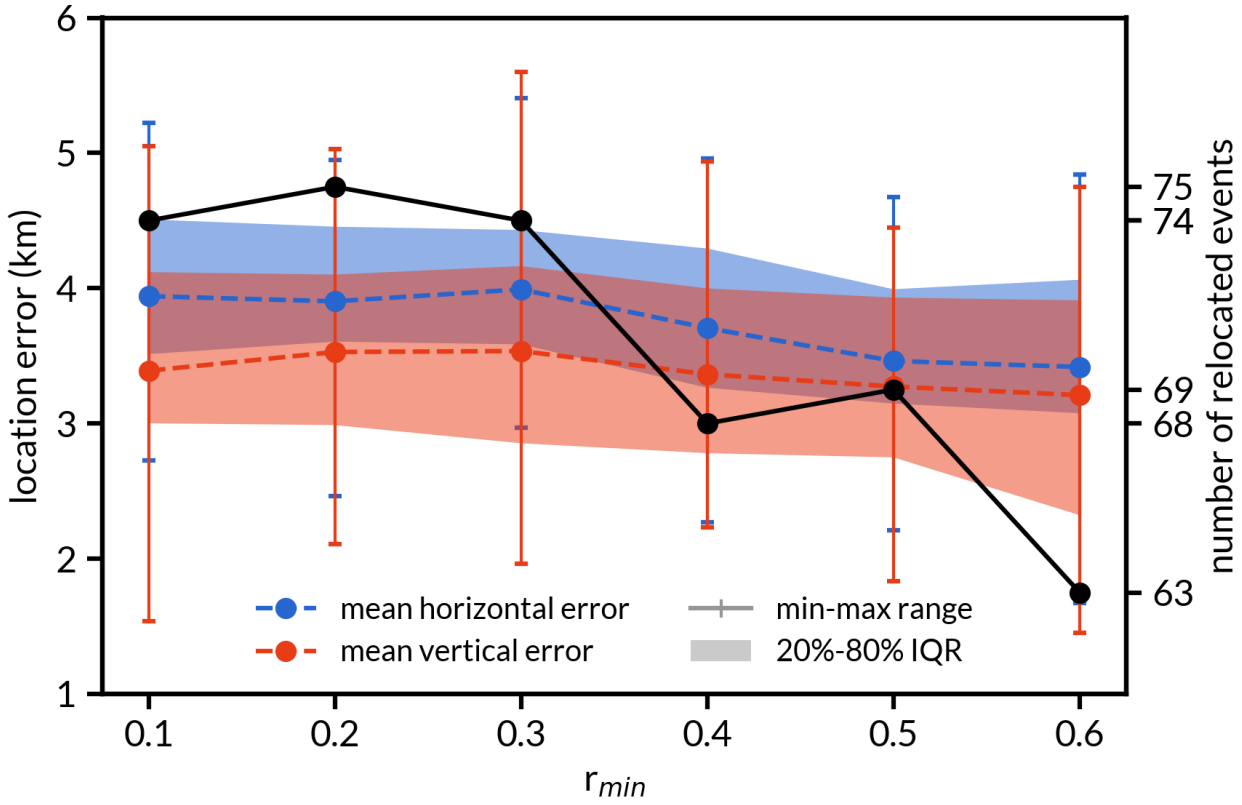

Figure S13. Distribution of GrowClust uncertainties as a function of the correlation threshold r_{min}.